Ridge Waveguide Polarizer with Finite and Stepped-Thickness Septum

Jens Bornemann, *Senior Member, IEEE*, and Vladimir A. Labay

Abstract—This contribution presents new design dimensions for the ridge waveguide septum polarizer. Emphasis is placed first, on including the finite septum thickness in the analysis; second, demonstrating its influence on the polarizer performance; third, including a stepped approach for extremely thick septa; fourth, optimizing components without the need for additional phase-adjusting structures; and fifth, providing the application engineer with some design guidelines. Examples for varying septum thickness and/or number of sections are given for C-, X-, R120-, Ku- and K-band applications. The analysis is based on an efficient mode-matching technique. Evolution-strategy methods are used for optimization. Both algorithms are translated into PC-operational software. Results are compared with previously published theoretical/experimental polarizer data and with a finite-element analysis, and are found to be in good agreement.

I. INTRODUCTION

THE STEPPED-SEPTUM polarizer in square waveguide technology is well known for its application as orthomode transducer, e.g., [1], and polarization measurement equipment [2]. For the design of this structure, the critical aspect is to simultaneously achieve low input reflection values of the TE_{10} and TE_{01} modes as well as a 90-degree phase shift between the two orthogonal electric field components. Both conditions translate into return loss, isolation and axial ratio, which are the quantities specified in practice for performance evaluation. The first design published [1] satisfied the input reflection criteria but required an additional dielectric-slab phase shifter to adjust the phase difference. Consequently, later designs, which were based on scaling of dimensions in [1] but lacking the component for phase adjustment, failed to produce an acceptable phase response [3], [4]. Recently, the phase linearization of this component has been attempted by adding a corrugated waveguide polarizer [5]. Results for a five-step design without additional phase adjustment are presented in [6], and investigations on stepped septums in a circular waveguide enclosure are reported in [7]. A stepped-notch design based on the ridge waveguide short-end effect [9] is shown to produce too much phase variation [8] over an acceptable bandwidth of ten percent.

Except for the original component in [1] and scaled versions thereof, dimensions of new stepped-septum designs have not been published so far. This is mainly owing to the fact that, once the thickness of the septum is considered, the field

rotation of the TE_{10} wave is extremely difficult to control simultaneously in magnitude and phase.

Therefore, to provide the design engineer with some guidelines, this paper presents optimized dimensions of stepped ridge waveguide polarizers which achieve excellent performance for bandwidths up to 20 percent. The paper discusses a constant-thickness or stepped-thickness septum [Fig. 1(a)] for medium and extremely thick separation walls between the rectangular waveguide ports. The design procedure is based on rigorous but efficient mode-matching methods and evolution-strategy optimization techniques [10]–[13]. Singular value decomposition is used to accurately solve the eigenvalue problem of the individual stepped-septum cross sections [14].

II. THEORY

The mode-matching technique is used for the analysis of the ridge waveguide polarizer. Since this procedure, which calculates the coupling matrices leading to the generalized scattering matrix of the four-port [cf., Fig. 1(a)], has already been described, e.g., in [10]–[12], only the modifications with respect to the ridge waveguide cross-section functions need to be presented here. In Section II-A [Fig. 1(b)], they are given by

$$T_{hn}^{IIa}(x,y) = A_n^{IIa} \cos\{k_{xn}^{IIa}x\} \cos\left\{\frac{n\pi}{b}y\right\} \Big/ \sqrt{1 + \delta_{0n}} \quad (1)$$

$$T_{en}^{IIa}(x,y) = D_n^{IIa} \frac{1}{k_{xn}^{IIa}} \sin\{k_{xn}^{IIa}x\} \sin\left\{\frac{n\pi}{b}y\right\} \quad (2)$$

and in Section II-B

$$T_{hm}^{IIb}(x,y) = A_m^{IIb} \begin{bmatrix} \frac{1}{k_{xm}^{IIb}}\sin\{k_{xm}^{IIb}(x-a/2)\} \\ \cos\{k_{xm}^{IIb}(x-a/2)\} \end{bmatrix}$$

$$\times \cos\left\{\frac{m\pi}{d-c}(y-c)\right\} \Big/ \sqrt{1 + \delta_{0m}} \quad (3)$$

$$T_{em}^{IIb}(x,y) = D_m^{IIb} \begin{bmatrix} \cos\{k_{xm}^{IIb}(x-a/2)\} \\ \frac{1}{k_{xm}^{IIb}}\sin\{k_{xm}^{IIb}(x-a/2)\} \end{bmatrix}$$

$$\times \sin\left\{\frac{m\pi}{d-c}(y-c)\right\} \quad (4)$$

where the upper and lower expressions in (3), (4) refer to a magnetic and electric wall, respectively, at $a/2$. Separation constants $k_{xn,m}^{IIa,b}$ are determined at the cutoff frequency ω_c of a mode and, therefore, are given by

$$\begin{bmatrix} (k_{xn}^{IIa})^2 \\ (k_{xm}^{IIb})^2 \end{bmatrix} = \omega_c^2 \mu_0 \varepsilon_0 - \begin{bmatrix} \left(\frac{n\pi}{b}\right)^2 \\ \left(\frac{m\pi}{d-c}\right)^2 \end{bmatrix}. \quad (5)$$

The ridge waveguide eigenvalue problem is solved by applying singular value decomposition which results in an accurate and stable algorithm [14]. For details on the analysis leading to the generalized scattering matrix of a single section, the reader is referred to [10]–[12]. For this work, however, a generalized impedance matrix approach is adopted, which is analoguous to the admittance formulation of [13] and results in faster algorithms than the scattering matrix technique because of fewer and purely real matrix inversions.

Finally, the generalized impedance matrices for even-mode [magnetic wall at $a/2$, Fig. 1(b)] and odd-mode (electric wall at $a/2$) analyses are converted [13] to the generalized scattering matrices $\underline{S}_e$ and $\underline{S}_o$, respectively. Let $S_{11e}, S_{12e}, S_{21e}, S_{22e}$, and $S_{44o}, S_{42o}, S_{24o}, S_{22o}$ be the fundamental-mode parameters of generalized scattering matrices $\underline{S}_e$ and $\underline{S}_o$, then the fundamental-mode four-port S-matrix of the septum polarizer [Fig. 1(a)] is given by

$$
S =
\begin{bmatrix}
S_{11e} & \frac{1}{\sqrt{2}}S_{12e} & \frac{1}{\sqrt{2}}S_{12e} & 0 \\
\frac{1}{\sqrt{2}}S_{21e} & \frac{1}{2}[S_{22e} + S_{22o}] & \frac{1}{2}[S_{22e} - S_{22o}] & \frac{1}{\sqrt{2}}S_{42o} \\
\frac{1}{\sqrt{2}}S_{21e} & \frac{1}{2}[S_{22e} - S_{22o}] & \frac{1}{2}[S_{22e} + S_{22o}] & -\frac{1}{\sqrt{2}}S_{42o} \\
0 & \frac{1}{\sqrt{2}}S_{24o} & -\frac{1}{\sqrt{2}}S_{24o} & S_{44o}
\end{bmatrix}.
\tag{6}
$$

Note that since $\underline{S}_e$ and $\underline{S}_o$ satisfy all conditions for generalized scattering matrices, e.g., [15], S in (6) is unitary. Return loss and isolation at the rectangular waveguide ports are calculated from S_{22} and S_{23} of (6). The axial ratio is obtained by combining the transmission coefficients to form the overall electric field at the common (square) waveguide port and calculating the extrema with respect to angular variation.

With the symmetry condition included, the software is operational on standard 486 PCs using double precision compilers. For the determination of the ridge waveguide eigenmodes, 15 expansion terms are usually sufficient, except in cases of extremely small slot widths where up to 50 expansion terms in Subsection II-A were used. The number of terms in Subsection II-B is taken according to the slot ratio $(d - c)/b$ [Fig. 1(b)]. In longitudinal direction, 25 TE modes yield sufficient convergence behavior for magnetic wall symmetry. The number of TM modes equals that of TE modes minus the number of TE_{mn} modes with either $m = 0$ or $n = 0$. Since the electric-wall analysis is not as critical as the magnetic-wall one, only 15 to 19 TE and respective TM modes are sufficient in this case. Under these conditions, the analysis of one set of parameters at 30 frequency samples requires 20 to 30 minutes on a 66 MHz 486 PC. More than 80 percent of this time is required to determine the eigenfunctions of the individual ridge waveguides involved.

Therefore, the CPU time required for optimization depends on whether only the section lengths are optimized—in this case, the ridge waveguide eigenvalue problem needs to be solved only once—or both section lengths l_i and slot widths s_i [cf., Fig. 1(c)]. Using a combination of both methods in an evolution-strategy optimization procedure, e.g., [10], the overall CPU time for the design of a four-section polarizer is approximately 15 hours on a 486 PC.
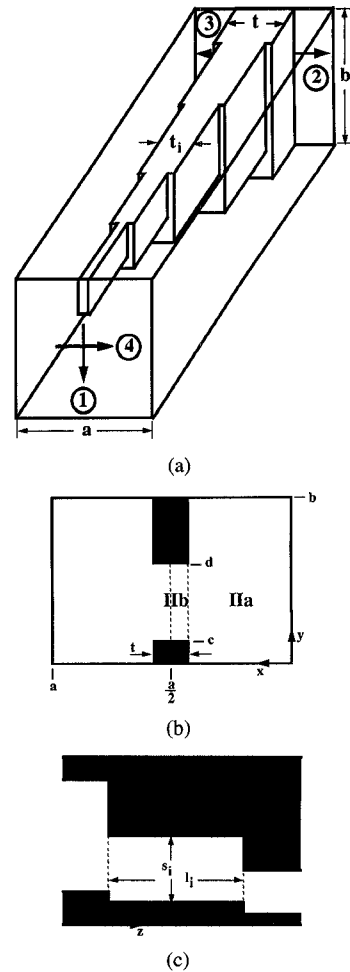

Fig. 1. Ridge waveguide polarizer with finite and stepped-thickness septum. (a) Position of septum in waveguide, (b) cross-section of ridge waveguide, (c) definition of slot width and section length.

For given return loss RL (dB), isolation IS (dB), M given frequency samples f_m, waveguide housing dimensions a, b, and septum thicknesses t_i, the parameters to be optimized are section lengths l_i and slot widths s_i in order to minimize the error function

$$
F = \sum_{m=1}^{M} u[RL - rl(f_m, l_i, s_i)]
$$
$$
+ u[IS - is(f_m, l_i, s_i)] + |90° - dp(f_m, l_i, s_i)| \tag{7}
$$

where $u[\ ]$ denotes a ramp multiplied by the unit step function, and $rl(), is()$, and $dp()$ are the actual return loss, isolation, and phase difference between the two orthogonal field components, respectively. It is obvious that this function will always maintain some positive value since the phase difference will never be exactly 90 degrees over a reasonable bandwidth. However, this parameter is the main contributor to a good axial ratio. Therefore, the optimization stops if the first two terms in (7) vanish and, in addition, a given axial ratio is obtained. It follows from (6) that return loss and isolation can be improved by adjusting the phases of the even-mode and odd-mode reflection coefficients. However, this can not be achieved independently of the transmission phases since the analysis is based on lossless twoports. It is obvious that,
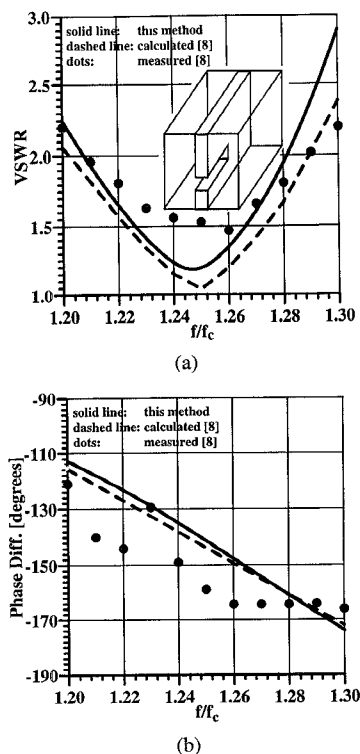
Fig. 2. Comparison of results of this method with theoretical and measured data of [8] at the example of a single-notch septum polarizer. (a) VSWR of TE_{10} mode; (b) phase difference between of orthogonal field components at square waveguide port.
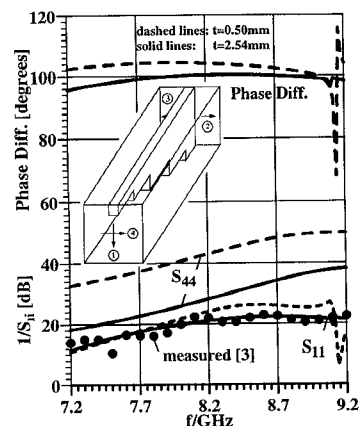

Fig. 3. Performance of four-section constant-thickness septum polarizer design in X-band waveguide. Septum thickness: $t = t_{1-4} = 0.5$ mm (dashed lines); $t = t_{1-4} = 2.54$ mm (solid lines); S_{11} measurements (o o o) [3].

once return loss and isolation exceed, say, 20 dB, the axial ratio almost exclusively depends on the (ideally, 90-degree) phase difference of the transmission coefficients.

The dimensions of septum polarizer structures given in the legends of this paper can be scaled into any other waveguide band. This is done by, first, calculating the midband-frequency-to-fundamental-mode-cutoff-frequency ratio of one of the configurations, say, with width $a = a_{old}$. Second, a new midband frequency is selected, and the ratio just calculated specifies the new waveguide width a_{new}. Finally, all dimensions of the polarizer (including the septum thicknesses) are multiplied by the ratio a_{new}/a_{old}. If certain dimensions, e.g., for the septum thickness, are not available, then the scaled values represent at least an excellent initial parameter set for further optimization. Most of the structures optimized during this work have been obtained from initial values calculated this way.

III. RESULTS

At the example of a single-section notch design, Fig. 2 shows a comparison between results obtained with this technique and measurements as well as calculations published in [8]. Although the septum thickness has been specified in [8] but has been neglected in the respective calculations, good agreement between the two theoretical data and, to a certain degree, measurements is obtained. However, the increased VSWR values produced by this method [Fig. 2(a), solid line] are certainly due to the finite septum thickness considered here. Since theoretical phase responses [Fig. 2(b)] agree quite well, it can be assumed that the deviations of the measured results

are caused by the measurement setup and not—as stated in [8]—by the finite septum thickness. It is worth mentioning that, although we are able to reproduce the phase response of the second structure presented in [8], a two-section notch design, agreement with the respective VSWR values could not be obtained.

Fig. 3 shows the performance of a four-section ridge waveguide polarizer with constant septum thickness. Measurements are taken from [3], where a scaled version of the design in [1] for X-band waveguide has been used, except for the fact that the septum thickness has been increased for stability. The scaled thickness is 0.5 mm (dashed lines) while the thickness obviously used in [3]—although not mentioned—is 2.54 mm (solid lines). This is evidenced not only by good agreement with the measured input return loss data of [3] but also by the fact that this thickness (0.1") is obtained if two X-band waveguides (0.9" × 0.4") are used as feeds for the polarizer setup. Three conclusions can be drawn from Fig. 3. First, the design is a scaled version of [1] and, therefore, shows an unacceptable phase-difference variation from the ideal value of 90 degrees so that either additional phase shifters are required, or an extremely poor axial ratio has to be accepted. (The corresponding axial ratio or phases are not shown in [3].) Second, the input reflection coefficients of both polarizations increase with increasing septum thickness, thus leading to lower return loss values. Third, the input return loss of port 1 and the transmission phase related to that port exhibit some resonance effects below the next higher-order mode cutoff (TE_{11} at 9.27 GHz). This fact has been experimentally verified in [6].

To make this design applicable for a satisfactory polarizer operation and still use the obvious septum thickness of 2.54 mm, the structure has been optimized—with slot widths and section lengths as optimization parameters—for 30 dB return loss, 25 dB isolation, and 0.5 dB axial ratio over the 1 GHz bandwidth (12 percent) of Fig. 3. The performance is shown in Fig. 4, and the optimized dimensions are given in the legend to Fig. 4. Also shown in Fig. 4 is the influence of the septum thickness. Since the structure has been optimized, any change in septum dimensions will deteriorate its performance.
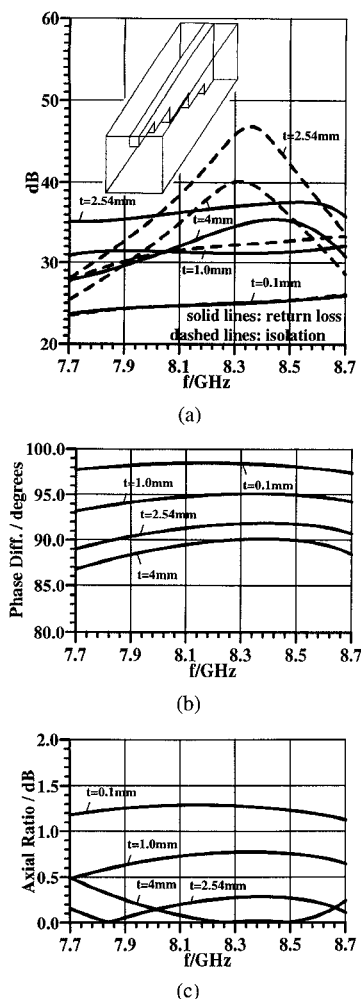
Fig. 4. Influence of septum thickness variation on four-section constant-thickness septum polarizer in X-band waveguide. Dimensions (optimized): $a = b = 22.86$ mm, $t = t_{1-4} = 2.54$ mm, $s_1 = 20.018$ mm, $s_2 = 15.545$ mm, $s_3 = 11.733$ mm, $s_4 = 5.928$ mm, $l_1 = 12.468$ mm, $l_2 = 11.474$ mm, $l_3 = 11.163$ mm, $l_4 = 3.619$ mm. (a) Return loss and isolation, (b) phase difference, and (c) axial ratio.

It is felt, however, that the dependence on septum thickness shown in Fig. 4 provides the design engineer with some useful guidelines as to what to expect if, e.g., in a scaled version of this design, the thickness required is not available or not manufacturable. In this respect, it is interesting to note that a relatively thin septum ($t = 0.1$ mm) results in a considerably degraded performance in axial ratio [Fig. 4(c)], whereas return loss and isolation values of better than 23.5 dB [Fig. 4(a)] might still be acceptable in practise. (Note that for thin septa, return loss and isolation are almost identical since the odd-mode contribution in (6) becomes negligibly small.) As the thickness increases ($t = 1.0$ mm), both return loss and isolation improve [Fig. 4(a)] up to the thickness used in the optimization ($t = 2.54$ mm). Of course, a further increase of septum thickness ($t = 4$ mm) results again in a performance degradation.

It is interesting to look at the corresponding phase difference and axial ratio behavior in Fig. 4(b) and (c), respectively. The phase difference of the two orthogonal field components at the common waveguide port decreases with increasing septum thickness [Fig. 4(b)]. With return loss and isolation values

better than 20 dB, it can be assumed that the transmission coefficients are close to unity and almost identical in magnitude. Consequently, their phase difference predominately determines the axial ratio [Fig. 4(c)] of the polarizer. It improves with the phase difference approaching 90 degrees and vanishes at exactly 90 degrees. From a practical point of view in this design example, it is important to notice that the thinnest septum investigated ($t = 0.1$ mm) leads to an unacceptably high axial ratio—as mentioned earlier—due to an approximately 8 degree phase error. Comparing the curves for $t = 1$ mm and 4 mm at 7.7 GHz in both Fig. 4(b) and (c), a maximum phase error of 3.3 degree is acceptable in this design axample to keep the axial ratio just below 0.5 dB.

The X-band waveguide housing used in Figs. 3 and 4 has a ridge-to-waveguide width ratio of $t/a = 0.11$ due to the cross-section dimensions of the two input waveguides. For standard K-band waveguides (0.42" × 0.17"), for instance, the resulting ratio is $t/a = 0.19$ which is far too high to obtain an acceptable polarizer performance. The classical solution to this problem is to carry out the polarizer design with a thinner septum and place additional discontinuities into the feeding rectangular waveguides for matching purposes. Indeed, this is probably the best method in order to maintain the specifications of the polarizer. However, it also adds additional length to the component which is often undesirable in practice. Therefore, we propose a compromise structure which slightly degrades the polarizer performance but has the advantage of maintaining the actual space requirements of the component. The idea is to incorporate the matching discontinuities into the polarizer section where they lead to a stepped-thickness design as depicted in Fig. 1(a). Fig. 5 shows the performance of such a design example for two K-band input waveguides (see legend to Fig. 5 for dimensions) and a ratio of only $t/a = 0.04$ at the common waveguide port. For given septum thicknesses and housing dimensions, slot widths and lengths of the ridge waveguide sections have been optimized for broadband performance. The bandwidth for 22 dB return loss/isolation and 0.5 dB axial ratio is better than 16 percent. For 25 dB return loss and isolation, this value reduces to 11 percent.

An even worse design scenario comes about if height-reduced waveguides (e.g., 0.25 : 1 instead of 0.5 : 1, as they are frequently employed in feed systems) are used as input ports. In this case, the septum can be of a thickness which equals the height of the original waveguide, i.e., $t/a = 0.5$. A design example for R120 waveguide using the stepped-thickness septum approach is given in Fig. 6. It is obvious that due to the relatively thick sections involved, return loss and isolation peaks become narrower, they clearly differ in frequency, and the axial ratio is not necessarily at its minimum at those frequencies. Consequently, the achievable bandwidth is only eight percent for 20 dB return loss/isolation and 0.5 dB axial ratio. Again, we would like to stress that this is an unusual case and that thin septums and additional transformer sections in the feeding waveguides are superior with respect to performance. However, the stepped-thickness option (no additional transformers) might be worth considering if system space is a critical issue.
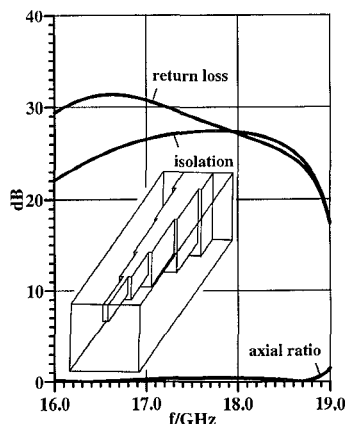
Fig. 5. Performance of an optimized four-section stepped-thickness septum polarizer design in K-band waveguide. Dimensions: $a = b = 10.668$ mm, $t = 2.032$ mm, $t_1 = 0.4$ mm, $t_2 = 0.8$ mm, $t_3 = 1.2$ mm, $t_4 = 1.6$ mm, $s_1 = 9.072$ mm, $s_2 = 7.177$ mm, $s_3 = 5.493$ mm, $s_4 = 3.679$ mm, $l_1 = 5.803$ mm, $l_2 = 5.445$ mm, $l_3 = 5.368$ mm, $l_4 = 1.755$ mm.
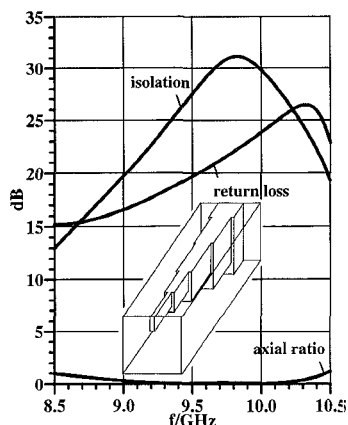

Fig. 6. Performance of an optimized four-section stepped-thickness septum polarizer design in R120 waveguide with reduced-height input ports. Dimensions: $a = b = 19.05$ mm, $t = 9.525$ mm, $t_1 = 1.0$ mm, $t_2 = 3.0$ mm, $t_3 = 5.0$ mm, $t_4 = 7.0$ mm, $s_1 = 15.935$ mm, $s_2 = 12.289$ mm, $s_3 = 8.899$ mm, $s_4 = 4.722$ mm, $l_1 = 10.009$ mm, $l_2 = 9.772$ mm, $l_3 = 7.971$ mm, $l_4 = 3.229$ mm.

Fig. 7 show the results of an investigation regarding the number of ridge waveguide sections in the polarizer design for a constant but fairly thick septum of $t/a = 0.14$. Note that return loss and isolation [Fig. 7(a)] peak at different frequencies which generally occurs if the septum thickness is not negligible. The two-section design $(N =) 2$ has fairly limited application as is obvious from the return loss, isolation and axial ratio behavior in Fig. 7(a) and (b), respectively. For a reasonable performance, at least a three-section design $(N =) 3$ should be used which simultaneously achieves 25 dB return loss/isolation and 0.5 dB axial ratio from 13.6 to 15 GHz. The corresponding values for the four-section design $(N =) 4$ are 12.9 to 15 GHz. Of course, a further increase of sections will increase the bandwidth, but only to a very small degree. The dependence of bandwidth gain on the number of sections is highly nonlinear and, therefore, the bandwidth cannot be significantly broadened by employing five or six sections. One reason for this is certainly the septum thickness. On the other
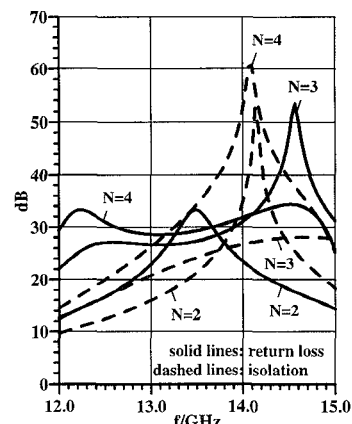
(a)
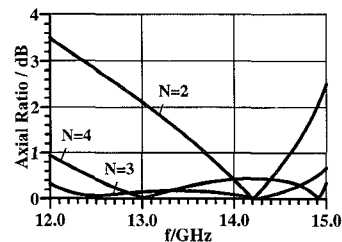
(b)

Fig. 7. Influence of the number of ridge waveguide sections on polarizer performance. Dimensions: $a = b = 13.5$ mm, $t = t_{1-4} = 1.86$ mm; $N = 2$: $s_1 = 9.330$ mm, $s_2 = 3.922$ mm, $l_1 = 6.539$ mm, $l_2 = 3.496$ mm; $N = 3$: $s_1 = 10.980$ mm, $s_2 = 7.633$ mm, $s_3 = 3.717$ mm, $l_1 = 7.759$ mm, $l_2 = 6734$ mm, $l_3 = 3.557$ mm; $N = 4$: $s_1 = 11.571$ mm, $s_2 = 9.126$ mm, $s_3 = 6.899$ mm, $s_4 = 3.465$ mm, $l_1 = 6.094$ mm, $l_2 = 6.214$ mm, $l_3 = 6.460$ mm, $l_4 = 2.323$ mm. (a) Return loss and isolation. (b) axial ratio.

hand, however, the principle of this polarizer requires it to be operated between the TE_{10} and TE_{11} mode cutoff frequencies of the common-port waveguide. Toward the TE_{10} cutoff, the high amount of dispersion complicates a broadband match while, toward the upper end, the high phase error (deviation from 90 degrees) between the two orthogonal field components (cf., Fig. 3 and measurements in [6]) shortly below TE_{11} cutoff leads to a degradation of the axial ratio performance.

In order to utilize most of the available bandwidth, the septum thickness has to be reduced so that a four-section polarizer is usually sufficient. A design example having $t/a = 0.02$ for C-band application is presented in Fig. 8. The bandwidth of 25 dB return loss/isolation and 0.5 dB axial ratio is 19 percent (3.47–4.2 GHz); 23 dB and 0.8 dB, respectively, are achieved over 21 percent, i.e., the entire frequency range of Fig. 8. An optimization of a five-section polarizer failed to significantly improve this performance. For comparison, Fig. 8 also displays the return loss data obtained by a finite-element analysis (HFSS) for vanishing strip thickness. The agreement is reasonable considering the fact that a septum thickness lower than that used for optimization ($t = 0.94$ mm) increases input reflection according to Fig. 4. Since the method presented here is unable to handle a vanishing septum thickness, while inclusion of the small but finite thickness in the finite-element method leads to astronomical CPU time requirements, we refrain from a comparison of results for exactly the same structure.
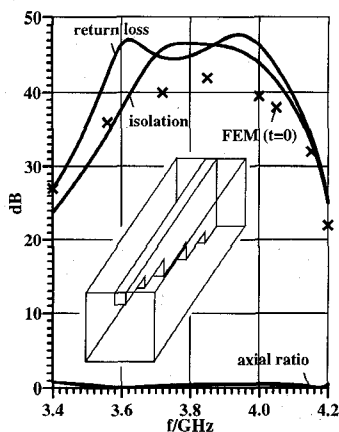
Fig. 8. Performance of an optimized four-section constant-thickness septum polarizer for C-band applications and comparison with finite-element analysis ($t = 0$). Dimensions: $a = b = 48.26$ mm, $t = t_{1-4} = 0.94$ mm, $s_1 = 41.045$ mm, $s_2 = 32.390$ mm, $s_3 = 24.278$ mm, $s_4 = 12.278$ mm, $l_1 = 25.589$ mm, $l_2 = 24.803$ mm, $l_3 = 24.232$ mm, $l_4 = 7.380$ mm.

IV. CONCLUSION

Mode-matching techniques based on electric and magnetic wall symmetry offer an attractive and—equally important—PC-operational solution for the computer-aided analysis and design of ridge waveguide septum polarizers. By rigorously taken the finite septum width into account, it is demonstrated that any variation of this thickness is to the detriment of the polarizer performance. For extreme wall thicknesses between the two feeding rectangular waveguides, a new stepped-thickness septum polarizer design is proposed as a compromise between performance specifications and component's space requirements. It is shown that four-section designs can cover most of the available bandwidth for reasonable performance specification and moderate septum thickness. The optimized dimensions given in the legends can be scaled for operation in different frequency ranges/waveguide housings. The method presented produces results in good agreement with previously published theoretical and experimental data.

REFERENCES

[1] M. H. Chen and G. N. Tsandoulas, "A wide-band square-waveguide array polarizer," IEEE Trans. Antennas Propagat., vol. AP-21, pp. 389–391, May 1973.

[2] H. E. Schrank, "Polarization measurements using the septum polarizer," in 1982 IEEE AP-S Int. Symp. Dig., pp. 227–230.

[3] T. Ege and P. McAndrew, "Analysis of stepped septum polarizers," Electron. Lett., vol. 21, pp. 1166–1168, Nov. 1985.

[4] L. S. Riggs, G. K. Gothard and F. J. German, "Transmission line matrix (TLM) modeling of a stepped-septum square-waveguide polarizer," in ACES '93 Conf. Proc., Mar. 1993, pp. 450–457.

[5] R. Ihmels, U. Papziner, and F. Arndt, "Field theory design of a corrugated septum OMT," in 1993 IEEE MTT-S Int. Microwave Symp. Dig., pp. 909–912.

[6] J. Esteban and J. M. Rebollar, "Field theory CAD of septum OMT-polarizers," in 1992 IEEE AP-S Int. Symp. Dig., pp. 2146–2149.

[7] R. Behe and P. Brachat, "Compact duplexer-polarizer with semicircular waveguide," IEEE Trans. Antennas Propagat., vol. 39, pp. 1222–1224, Aug. 1991.

[8] N. C. Albertsen and P. Skov-Madsen, "A compact septum polarizer," IEEE Trans. Microwave Theory Tech., vol. MTT-31, pp. 654–660, Aug. 1983.

[9] Y. Konishi and H. Matsumura, "Short end effect of ridge guide with planar circuit mounted in a waveguide," IEEE Trans. Microwave Theory Tech., vol. MTT-27, pp. 168–170, Feb. 1979.

[10] J. Bornemann and F. Arndt, "Transverse resonance, standing wave, and resonator formulations of the ridge waveguide eigenvalue problem and its application to the design of E-plane finned waveguide filters," IEEE Trans. Microwave Theory Tech., vol. 38, pp. 1104–1113, Aug. 1990.

[11] J. Bornemann, "Comparison between different formulations of the transverse resonance field-matching technique for the three-dimensional analysis of metal-finned waveguide resonators," Int. J. Numerical Modeling, vol. 4, pp. 63–73, Mar. 1991.

[12] J. Bornemann and F. Arndt, "Modal S-matrix design of metal finned waveguide components and its application to transformers and filters," IEEE Trans. Microwave Theory Tech., vol. 40, pp. 1528–1537, July 1992.

[13] F. Alessandri, G. Bartolucci and R. Sorrentino, "Admittance matrix formulation of waveguide discontinuity problems: Computer-aided design of branch guide directional couplers," IEEE Trans. Microwave Theory Tech., vol. 36, pp. 394–403, Feb. 1988.

[14] V. A. Labay and J. Bornemann, "Singular value decomposition improves accuracy and reliability of T-septum waveguide field-matching analysis," Int. J. Microwave Millimeter-Wave Computer-Aided Engineering, vol. 2, pp. 82–89, Apr. 1992.

[15] H. D. Knetsch, "Beitrag zur Theorie sprunghafter Querschnittsveränderungen von Hohlleitern," Arch. Elektr. Uebertr., vol. 22, no. 12, pp. 591–600, 1968.

Jens Bornemann (M'87–SM'90) was born in Hamburg, Germany, on May 26, 1952. He received the Dipl.-Ing. and the Dr.-Ing. degrees, both in electrical engineering, from the University of Bremen, Germany, in 1980 and 1984, respectively.

From 1980 to 1983, he was a Research and Teaching Assistant in the Microwave Department at the University of Bremen, where he worked on quasi-planar waveguide configurations and computer-aided E-plane filter design. In 1985, after a two-year period as a Consulting Engineer and Lecturer, he joined the University of Bremen again and was employed at the level of Assistant Professor. Since April 1988, he has been with the University of Victoria, Victoria, B.C., Canada, where he is currently a Professor in the Department of Electrical and Computer Engineering. His research activities include microwave/millimeter-wave components and systems design, and problems of electromagnetic field theory in integrated circuits and radiating structures. He is a coauthor of Waveguide Components for Antenna Feed Systems. Theory and Design (Artech House, 1993) and has authored/coauthored more than 90 technical papers. He is a Registered Professional Engineer in the Province of British Columbia, Canada.

Dr. Bornemann was one of the recipients of the A.F. Bulgin Premium of the Institution of Electronic and Radio Engineers in 1983. He is a Fellow of the British Columbia Advanced Systems Institute and serves on the editorial boards of the IEEE TRANSACTIONS ON MICROWAVE THEORY AND TECHNIQUES and the International Journal of Numerical Modelling.

Vladimir A. Labay was born in Winnipeg, Manitoba, Canada on May 11, 1965. He earned the B.S. in engineering (B.Sc.E.E.) and the M.S. degree at the University of Manitoba in 1987 and 1990, respectively. Presently, he is a Ph.D. candidate in the Department of Electrical Engineering at the University of Victoria, Victoria, British Columbia.

His current research interests include numerical modeling of microwave and millimeter-wave components with emphasis on the characterization of arbitrarily shaped discontinuities within rectangular waveguides.